IOPscience iopscience.iop.org

Home Search Collections Journals About Contact us My IOPscience

Measurement of rotor centre flow direction and turbulence in wind farm environment

This content has been downloaded from IOPscience. Please scroll down to see the full text.

2014 J. Phys.: Conf. Ser. 524 012167

(http://iopscience.iop.org/1742-6596/524/1/012167)

View the table of contents for this issue, or go to the journal homepage for more

Download details:

IP Address: 130.225.93.211
This content was downloaded on 26/08/2014 at 13:45

Please note that terms and conditions apply.

Measurement of rotor centre flow direction and turbulence in wind farm environment

T F Pedersen[1], G Demurtas[1], A Sommer[2] and J Højstrup[3]

[1] DTU Wind Energy, Risø Campus, Bldg 125, Frederiksborgvej 399, 4000 Roskilde, DK
[2] Vattenfall, Oldenborggade 25-31, 7000 Fredericia, DK
[3] Wind Solutions, Langballevej 27c, 8320 Maarslet, DK

E-mail: trpe@dtu.dk, giod@dtu.dk, anders.sommer@vattenfall.com, jhojstrup@wind-solutions.com

Abstract. The measurement of inflow to a wind turbine rotor was made with a spinner anemometer on a 2 MW wind turbine in a wind farm of eight wind turbines. The wind speed, yaw misalignment and flow inclination angle was measured during a five months measurement campaign. Angular measurements were calibrated by yawing the wind turbine in and out of the wind in stopped conditions. Wind speed was calibrated relative to a met mast in a wake-free wind sector during operation. The calibration measurements were used to determine the basic k_1 and k_2 constants of the spinner anemometer and a four parameter induction factor function. Yaw measurements and turbulence measurements, where the average wind speed was corrected to the far field with the induction function, showed good correlation with mast measurements. The yaw misalignment measurements showed a significant yaw misalignment for most of the wind speed range, and also a minor symmetric yaw misalignment pattern. The flow inclination angle showed slight variation of inflow angle with wind speed and clear wake swirl patterns in the wakes of the other wind turbines. Turbulence intensity measurements showed clear variations from low turbulence in the wake-free wind sector to high turbulence in the wakes of the other wind turbines.

1. Introduction

The measurement of inflow to the wind turbine rotor is of relevance for control purposes and for performance and loads assessment. Yaw misalignment of turbines is traditionally made with reference to a met mast, but newer instruments are being applied. Yaw misalignment and flow inclination angle measurements with a spinner anemometer was made from 2007 [1, 2, 3]. Yaw measurements with a spinner based lidar was compared with mast measurements in [4], and shortcomings were discussed in [5]. Yaw measurements with a spinner anemometer were compared with nacelle based lidars [6]. Turbulence measurements with nacelle based lidars show some deviation from mast measurements due to long measurement volume [7]. Turbulence measurements with a spinner anemometer is new. Appropriate calibration of a spinner anemometer show that with correction for induction, turbulence measurements can be made with high confidence. Thus qualitative measurements in a wind farm of these measurement parameters can reveal new insight into the wind inflow to wind turbine rotors.

Content from this work may be used under the terms of the Creative Commons Attribution 3.0 licence. Any further distribution of this work must maintain attribution to the author(s) and the title of the work, journal citation and DOI.
Published under licence by IOP Publishing Ltd

2. Wind farm environment

The measurements were made on wind turbine no. 5 in Tjæreborg wind farm, see figure 1. The wind turbine is a V80 2 MW wind turbine with hub height 60 m and rotor diameter 80 m. The other wind turbines in the wind farm are Vestas and NEG Micon types with a nominal power of 2-2.75 MW and rotor diameters of 54-80 m. The reference met mast was located 120 m south-west (213°) of the no. 5 turbine. Cup anemometers and wind vanes were mounted on booms at hub height. A spinner anemometer was mounted on the spinner, see figure 2. Directions and relative distances are shown in table 1. The wake-free sector ($212° - 252°$) with the mast in front of wind turbine no. 5 was used for calibration purposes. The terrain in the sector was flat and without obstacles, with 1 km to the North sea. Another wake-free sector ($297° - 95°$) points towards open farmland but with the high surface roughness village Tjæreborg 1 km away in sector $300° - 330°$.

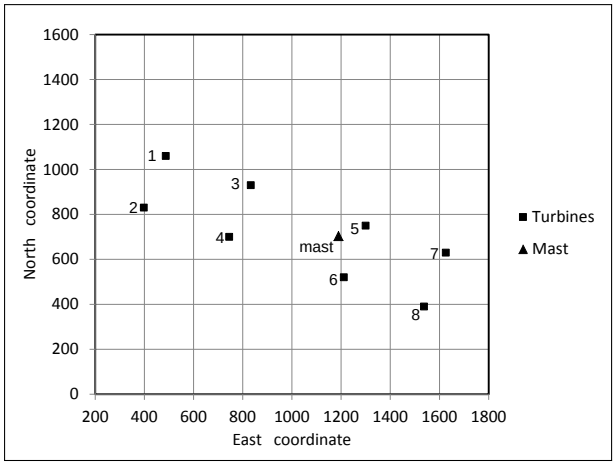

Figure 1. Wind farm layout of Tjæreborg wind farm with V80 test turbine no. 5.

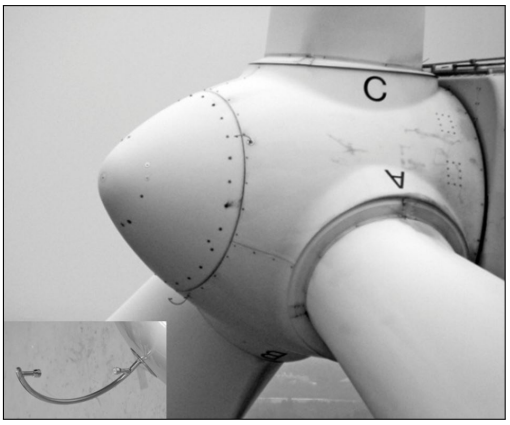

Figure 2. The spinner of the V80 wind turbine with sonic sensors mounted just behind nose cone assembly.

3. Calibration

The spinner anemometer algorithm utilizes two constants k_1 and k_2 to convert the measured wind speeds of the three sonic sensors to horizontal wind speed, yaw misalignment and flow inclination angle. The default values of the constants before calibration were set to $k_{1,d} = k_{2,d} = 1$. The calibration of angular measurements is dependent on the constant $k_\alpha = k_2/k_1$, the ratio between the two basic constants. For calibration of angular measurements one has to find a correction factor F_α to correct the default ratio to the corrected ratio $k_\alpha = F_\alpha k_{\alpha,d}$. k_1 may then be kept constant and k_2 be corrected to $k_2 = F_\alpha k_{2,d}$. The calibration for angular measurements is made by yawing the wind turbine in and out of the wind in stopped condition while measuring yaw misalignment and the nacelle direction with a yaw direction sensor. Figure 3 shows a plot of yaw direction data versus yaw misalignment data obtained during yawing. Figure 4 shows the time series after applying the correction to the yaw misalignment data. The correction factor $F_\alpha = 1.023$ is close to 1, and then the angular measurement data can be corrected proportionally, while otherwise the correction would have to take the non-linear conversion algorithm into account:

$$\alpha = \arctan(\frac{1}{F_\alpha} \tan \alpha_d) \approx \frac{\alpha_d}{F_\alpha} \tag{1}$$

Table 1. Relative directions and distances from wind turbines in the wind farm to the mast and to wind turbine no. 5. Wake sector is based on simple geometry.

Wind turbine no.	Distance to WT no.5	Direction to WT no. 5	Wake sector
1	10.9	291°	288°-293°
2	11.3	275°	273°-278°
3	6.3	291°	287°-296°
4	7.0	265°	261°-269°
5	0.0	-	-
6	3.2	201°	192°-210°
7	4.3	110°	104°-117°
8	5.4	147°	141°-152°
Wind turbine no.	Distance to mast	Direction to mast	Wake sector
1	9.8	297°	294°-300°
2	10.0	279°	276°-282°
3	5.3	302°	297°-308°
4	5.6	270°	264°-275°
5	1.5	67°	49°-85°
6	2.3	173°	161°-186°
7	5.5	100°	94°-105°
8	5.8	132°	127°-137°

Here α is the calibrated inflow angle to the rotor shaft and α_d the measured inflow angle with the default constants $k_{1,d} = k_{2,d} = 1$. The tilt angle of the wind turbine was for this calibration case neglected and the yaw misalignment was equalled the inflow angle to the rotor shaft.

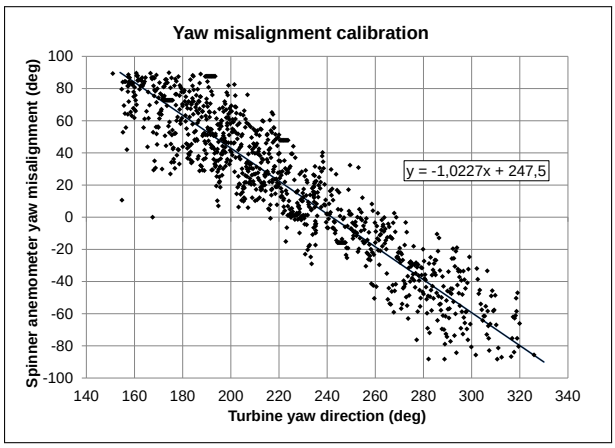

Figure 3. Plot of calibration data from yawing the wind turbine in and out of the wind.

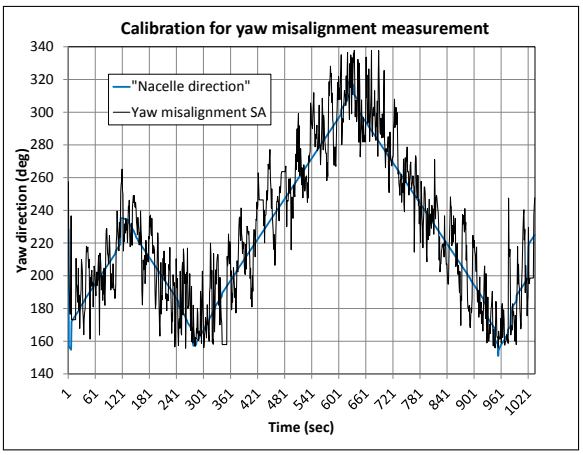

Figure 4. Plot of data from yawing with application of correction factor $F_\alpha = 1.023$.

The yaw misalignment measured with the spinner anemometer were compared to yaw misalignment measurements with the mast wind vane and yaw direction sensor, see figure 5. Except for a large 42° offset error of the yaw direction sensor seen in the figure, the slope shows

good agreement between the two measurement methods.

Calibration for wind speed measurements was made by relating spinner anemometer wind speed to a mast cup wind speed. Calibration could be made in stopped condition but this would imply high production losses. The measurements were instead made during operation. However, the mast distance was only 1.5D instead of the minimum required 2D, so the far field wind speed might be considered about 2% too low due to induction of the rotor.

The correction factor $F_1 = 0.743$ was determined to correct the spinner anemometer constants to measurement of the free wind speed in stopped condition, $k_1 = F_1 k_{1,d}$ and $k_2 = F_1 F_\alpha k_{2,d}$. Due to the fact that the angular correction factor F_α was very close to 1, the measured wind speed by the spinner anemometer U can with a good approximation be linearly related with the default measured wind speed U_d:

$$U = U_d \frac{1}{F_1} \frac{\cos \alpha_d}{\cos \alpha} \approx U_d \frac{1}{F_1} \tag{2}$$

Spinner and mast wind speed measurements during operation are shown in figure 6. The correction factor $F_1 = 0.743$ was determined by fitting data to very low and very high wind speeds, where the induced wind speed due to the operating rotor is insignificant. Figure 7 shows the data after application of the wind speed calibration correction factor according to equation 2.

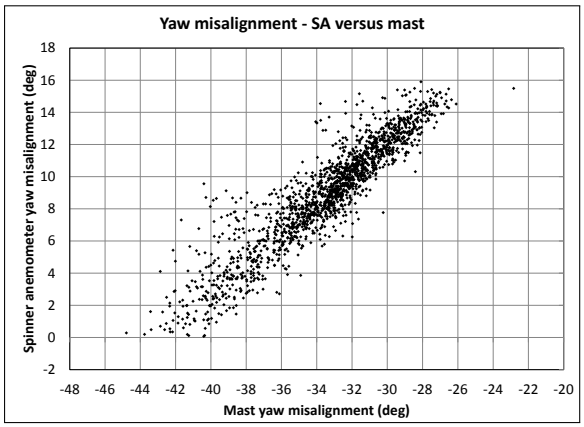

Figure 5. Yaw misalignment with spinner anemometer after calibration versus mast wind vane minus yaw direction (10 min mean).

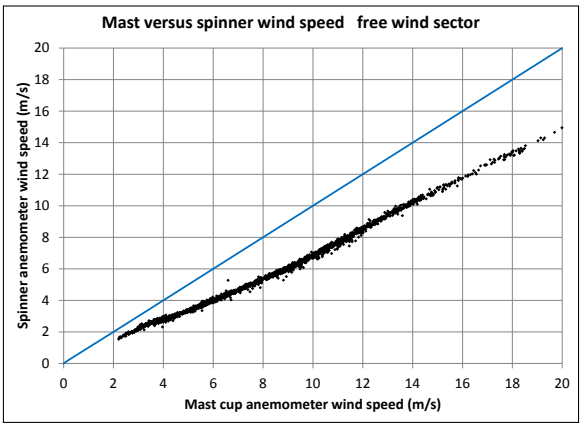

Figure 6. Spinner anemometer wind speed before applying F_1 correction factor versus mast cup wind speed (10 min mean).

The non-linearity of the curve in figure 7 is due to the rotor induced wind speed in the centre of the rotor during operation. The induction factor $a = (U_{cup} - U)/U_{cup}$, extracted from figure 7, is shown in figure 8. The induction factor data were fitted to an appropriate induction factor function with four parameters:

$$a = B(\frac{U - C}{A})^{D-1} \exp(\frac{U - C}{A})^D \tag{3}$$

The induction factor function with the parameters $A = 5.6$, $B = 0.25$, $C = 3$ and $D = 1.8$ is shown in blue in figure 8. Spinner anemometer wind speed data, corrected with the induction factor function, see figure 9, shows that corrected spinner anemometer wind speed comply well with free mast cup wind speed.

The standard deviation of the measured wind speeds with the spinner anemometer and the mast cup anemometer are plotted in figure 10 (without corrections for induction). The figure

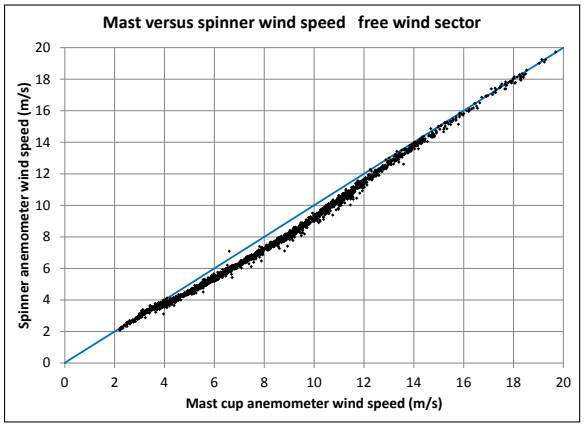

Figure 7. Spinner anemometer wind speed after applying $F_1 = 0.743$ correction factor versus mast cup wind speed (10 min mean).

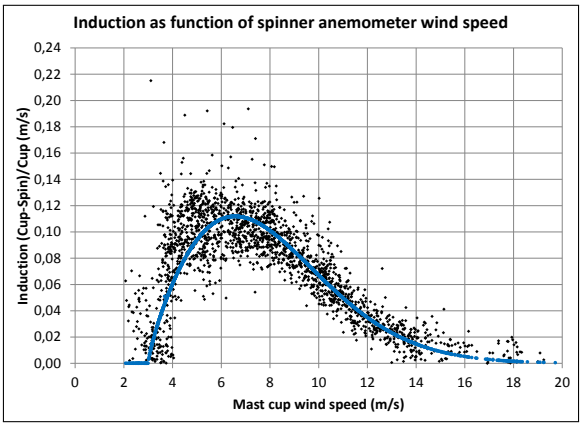

Figure 8. Induction factor scatter plot and fitted induction factor function in red, see equation 3 (10 min mean).

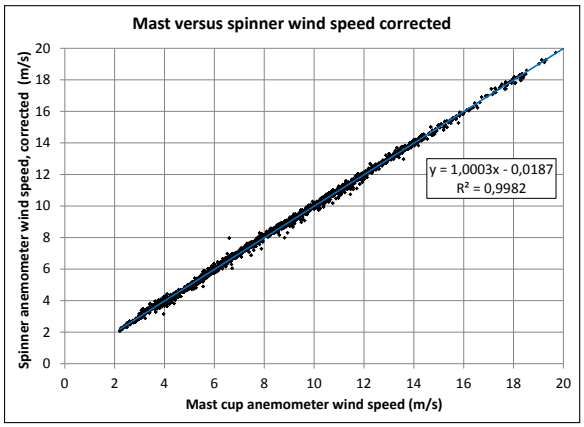

Figure 9. Spinner anemometer wind speed, corrected for induction versus mast cup wind speed (10min mean).

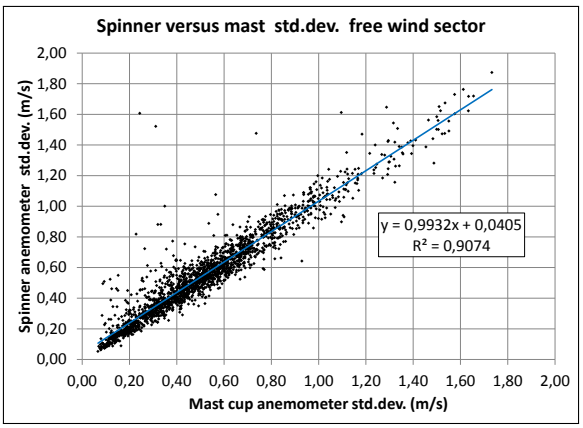

Figure 10. Spinner anemometer wind speed standard deviation versus mast cup wind speed standard deviation

shows good compliance between the spinner anemometer and mast measurements. However, the turbulence intensity measured by the spinner anemometer, see figure 11, is overestimated compared to the mast measurements. If we, meanwhile, correct the measured average wind speeds by the spinner anemometer to the far field average wind speed with the induction factor function, then the turbulence intensity measurements comply quite well with the mast cup measurements, see figure 12. This will be further commented in the discussion chapter. For all turbulence intensity measurements by the spinner anemometer, which are presented in the following, the average wind speed is corrected in this way to the far field while the standard deviation is not.

4. Inflow measurements from all wind directions

Inflow measurements from all wind directions are shown in figures 13 to 15. The yaw misalignment measurements, figure 13, show a rather scattered pattern, averaged at about 10°. Some scattered points go to negative yaw misalignments, and in the sector $300° - 330°$ a smaller cloud of data are centred around $-10°$. The flow inclination angle in figure 14 shows inflow angles scattered around 0°, which should be expected for flat terrain, but with significant up and down

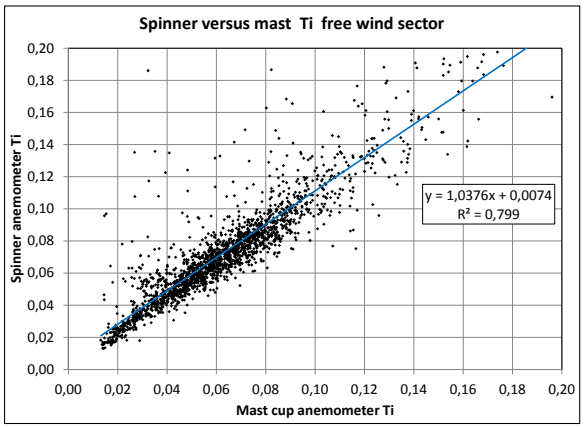

Figure 11. Spinner anemometer turbulence intensity versus mast cup turbulence intensity.

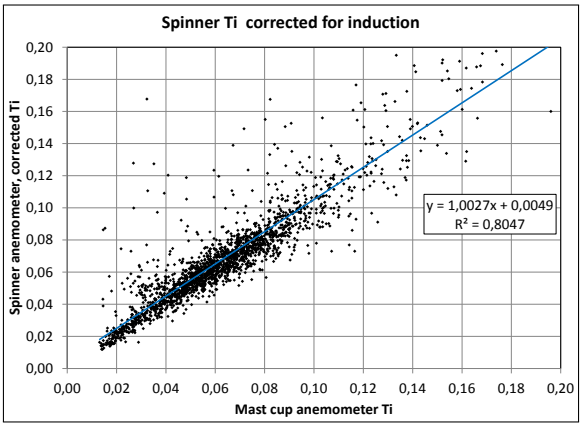

Figure 12. Spinner anemometer turbulence intensity corrected for induction versus mast cup turbulence intensity.

slopes in the sector $180° - 215°$, which corresponds to the wake of wind turbine no. 6. Minor up and down slopes are seen for the wakes of other wind turbines. Some sectors $300° - 330°$, $0° - 15°$ and $105° - 125°$ reach flow inclination angles of $-10°$. The turbulence measurements in figure 15 show significant changes behind the wakes of the different wind turbines in the wind farm. Most significant behind wind turbine no. 6 ($180° - 215°$), but also turbines no. 3 ($90° - 130°$), 4 ($130° - 155°$), 8 ($255° - 275°$) and 7 ($275° - 300°$). The maximum turbulence of 0.25 is seen behind turbine no. 6, while the turbulence behind the other wind turbines seem to be about the same 0.20. Figure 15 also shows the low turbulence in the wake-free calibration sector $212° - 252°$ and the high turbulence in the wake-free, high surface roughness sector $300° - 330°$.

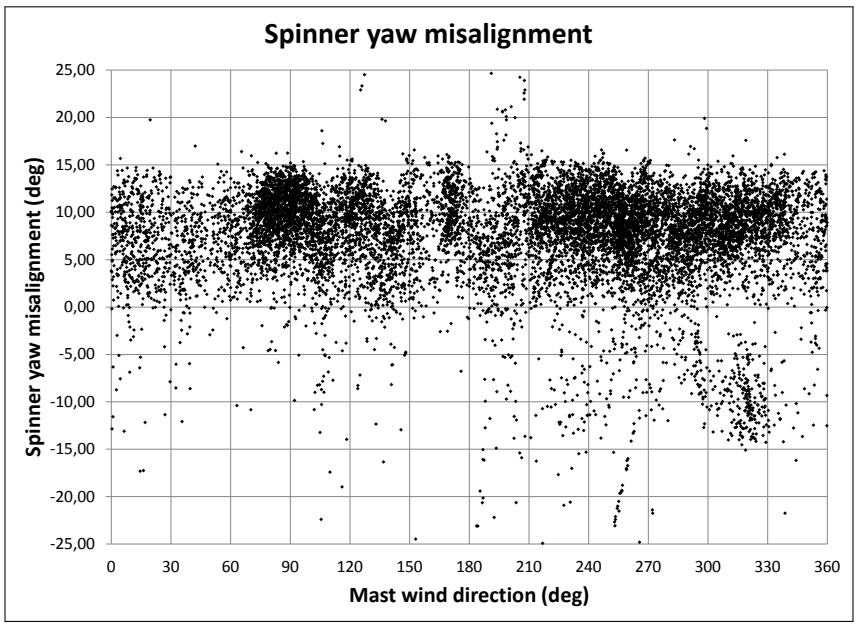

Figure 13. Spinner anemometer yaw misalignment measured for all wind directions (10min mean)

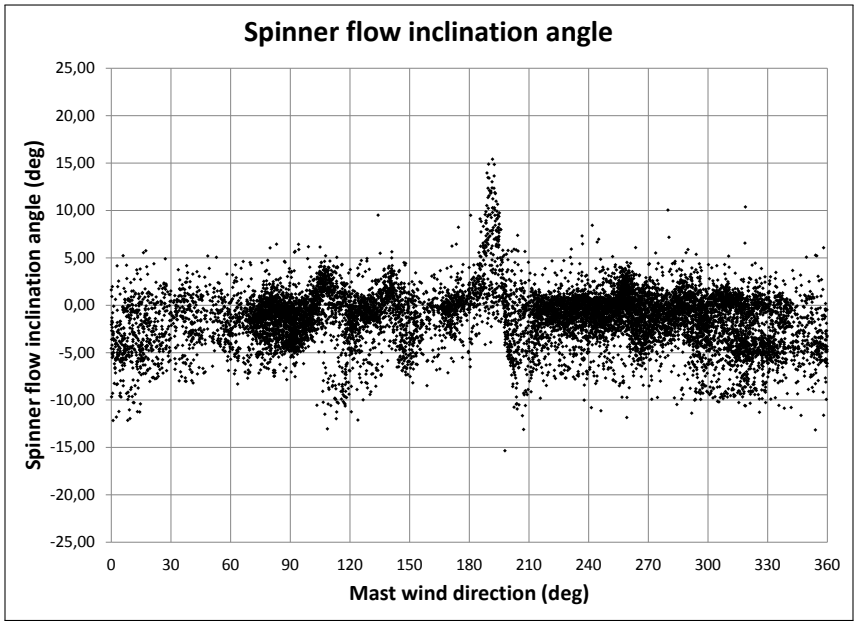

Figure 14. Spinner anemometer flow inclination angle measured for all wind directions (10min mean)

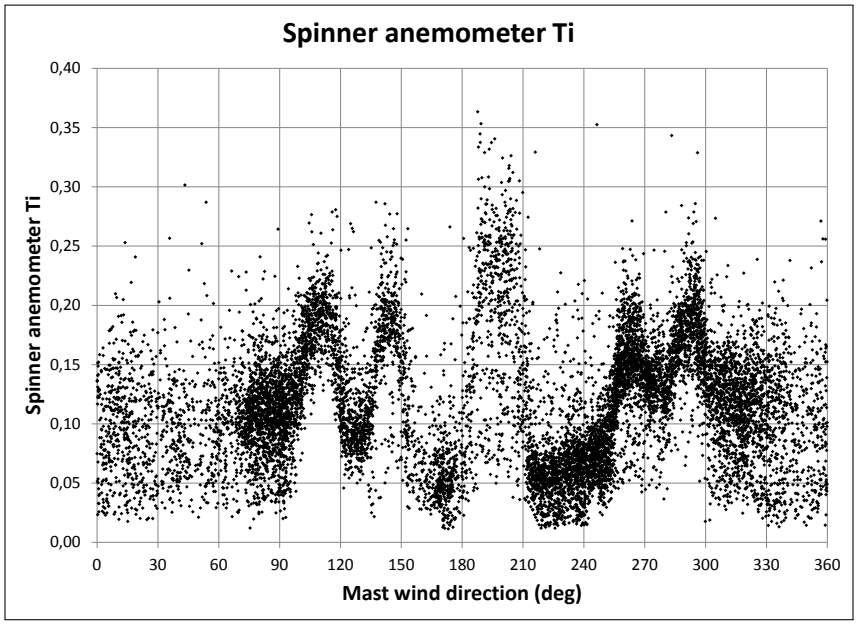

Figure 15. Spinner anemometer turbulence intensity measured for all wind directions (10min mean)

5. Inflow measurements as function of wind speed

The inflow measurements as function of wind speed are shown for the wake-free calibration sector in figures 16, 18 and 20. Measurements from all directions are shown in figures 17, 19 and 21.

The yaw misalignment in the wake-free sector in figure 16 is seen to increase from 3 m/s to a maximum of about 12° at 11 m/s, and is then decreased to about 8° at 18 m/s. A small number

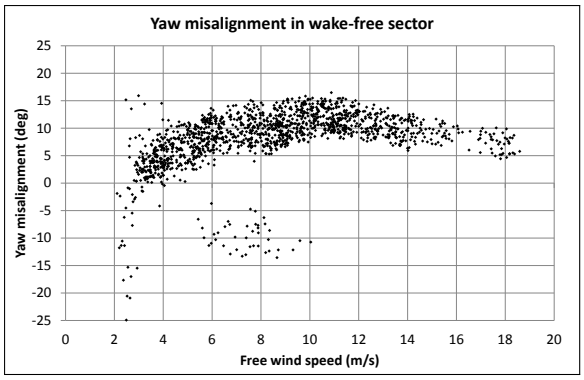

Figure 16. Yaw misalignment in wake-free sector

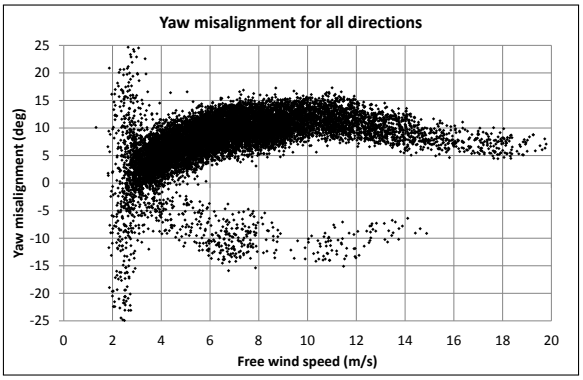

Figure 17. Yaw misalignment for all wind directions

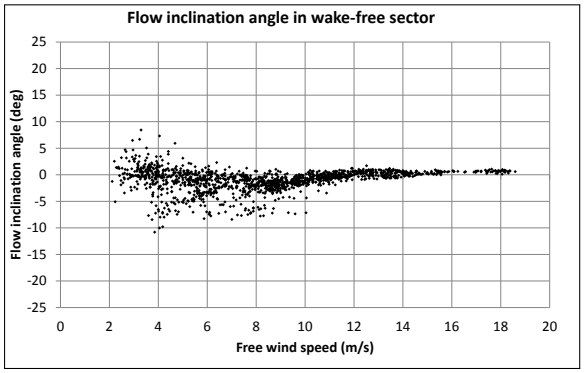

Figure 18. Flow inclination angle in wake-free sector

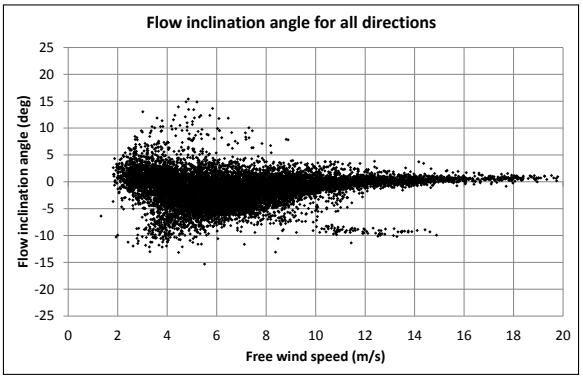

Figure 19. Flow inclination angle for all wind directions

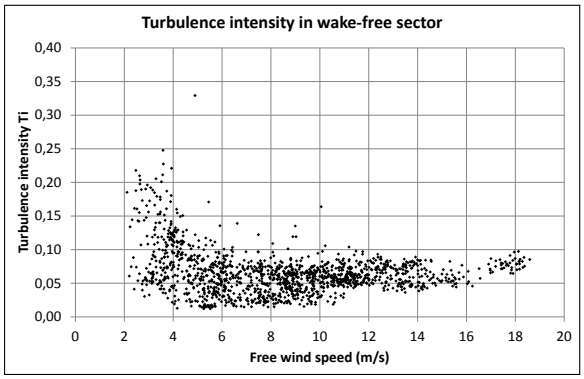

Figure 20. Turbulence intensity in wake-free sector

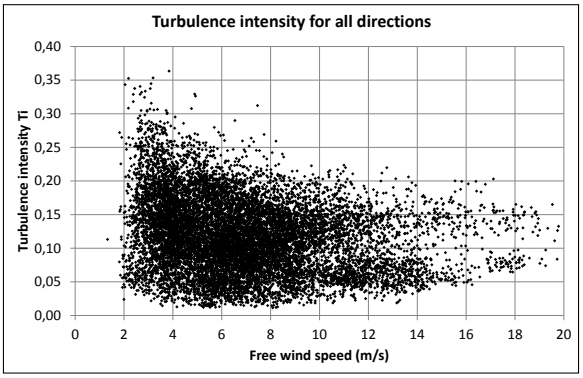

Figure 21. Turbulence intensity for all wind directions

of measurement points in the wind speed range 5-10 m/s are seen at a yaw misalignment of about $-10°$. For all wind directions, figure 17, the yaw misalignment measurements follow the same pattern but with an increase of measurement points at $-10°$. The flow inclination angle in the wake-free sector in figure 18 is close to $1°$ (positive upwards) in most of the wind speed range, but has a smaller dip in the range 5-10 m/s. A number of measurement points are scattered around $-5°$ in the wind speed range 4-10 m/s. For all wind directions, figure 19, the scatter of

the data is increased, but additionally some flow inclination angles at about $-8°$ is seen at 10-14 m/s wind speed. The turbulence intensity in the wake-free sector, figure 20, is seen to be below 8% in the wind speed range 6-18 m/s and is increased at lower wind speeds. The minimum turbulence intensities are close to 2%. For all wind directions the turbulence intensity, figure 21, is increased and for high wind speeds is averaged about 15%. Below 10 m/s the turbulence gradually increases up to 30%.

6. Discussion

The calibration of the spinner anemometer was made in a wake-free sector with low turbulence, and the calibration was shown to result in measurements that correspond quite well with the mast measurements. This was the case for angular measurements, figure 5, as well as for wind speed, figure 9, and turbulence measurements, figure 12. The preconditions for this qualitatively good result should be found in the low flow distortion on the sonic sensors in front of the rotor and in the fact that the turbulence intensity is only disturbed by the overall induction due to the rotor. In defining the wind speed measured by the spinner anemometer as the free wind speed in stopped condition the induction becomes a clean correction that only depend on rotor parameters such as rotational speed, pitch angle and rotor thrust. Local distortion effects that nacelle based instruments are very dependent on can be neglected even though the spinner anemometer sonic sensors are influenced by the blade root vicinity. As long as the spinner anemometer configuration applies to the spinner anemometer conversion algorithm the calibration should lead to adequate calibration results. Measurement of free wind speed requires the induction function to be applied, and this can be made with a simple function with four constants. Applying the induction function, turbulence measurements can also be made with good accuracy. The standard deviation measured by the mast and the spinner anemometer, figure 10, seems to correlate quite well. However, the average wind speed has to be adjusted to the free wind. The reason for this must be that the smaller vortices that dominates the standard deviation, measured by the spinner anemometer, are not affected by the rotor induced wind speed, while the average speed of the overall flow is reduced due to the induction. The question is whether this will always be the case independent of the structure of the turbulence.

The measurements of rotor centre inflow shown in figures 13 to 21 show features that need to be commented. The clear up and down slope of flow inclination angles in the sector $180°$ to $215°$ in figure 14 is very distinct. This wind sector is the wake sector of the nearest wind turbine no. 6 3.2 rotor diameters away. The flow inclination pattern is well explained by the swirl of the wake of the upfront wind turbine. The direction of rotation of its rotor is CW (seen from the front). This causes a wake swirl in the opposite CCW direction, and this gives the peak tip flow inclination angles of $-13°$ and $15°$, based on 10 min averages. Minor wake swirls are seen behind the other wind turbines. The wake swirl based on 30 sec averages is shown in figure 22. The shorter time average data show a more robust cluster of data for the wake swirl where the slope on the up-going inclination angles seem to be quite much the opposite of the down-going angles.

The yaw misalignment, figure 13, shows a smaller amount of data at about $-10°$ in the sector $300°$ to $330°$. This sector is a wake-free sector but with high turbulence due to the nearby village Tjæreborg about 1 km away. Figure 17 reveals that the $-10°$ yaw misalignment actually occurs at quite high wind speeds, 10-14 m/s. The figure also shows that a symmetric yaw misalignment pattern exists for a smaller amount of data. The cause of this might be due to the control system making alternating use of the two 2D sonics that are symmetrically mounted on either side of the nacelle of the wind turbine. The log on the wind turbine might confirm this assumption as irregularities on the yaw control were identified during the measurement campaign.

The yaw misalignment of $-10°$ in the sector $300°$ to $330°$ is observed to occur at the same time as a $-10°$ flow inclination angle at 10-14 m/s, see figures 17, 19 and 14. A closer look at

the wind inflow from the 300° to 330° sector with 30 sec averaging data, see figure 23, shows that the yaw misalignment and flow inclination angle are not correlated, but are divided into two distinct scattered groups. It is surprising to see the high scatter in flow inclination angles, especially the very low downwards values. The explanation to these very low values may be due to the high terrain roughness from the village very close to the wind turbine. The drag of the village reduces the wind speeds at lower levels which might give room for air with higher wind speeds from above to enter lower levels.

Evidence of faulty measurements of the spinner anemometer have been considered but there have not been found reasons for rejecting unexpected inflow angular measurements. Measurements of inflow angles in the centre of a wind turbine rotor in wind farm environment was never measured before, so hopefully physical explanations for the explored phenomena will be found by other means to support the measurements.

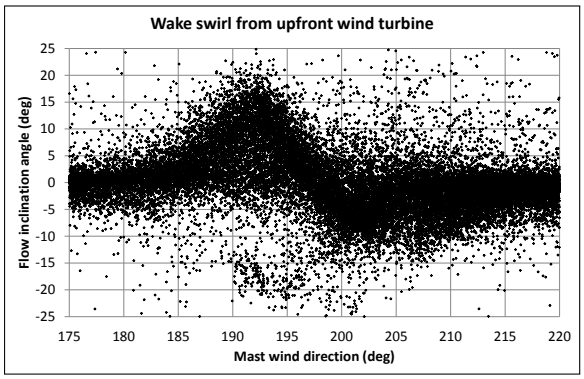

Figure 22. Plot of flow inclination angle in the wake sector behind turbine no. 6 (30sec mean)

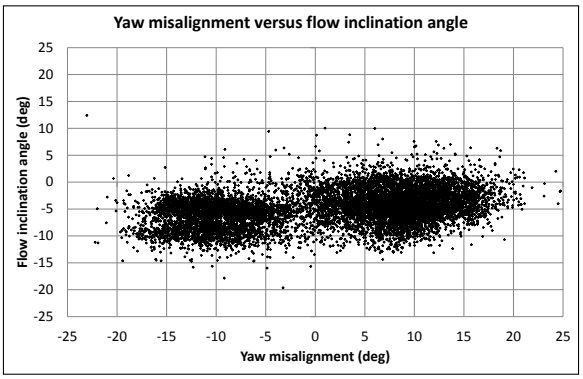

Figure 23. Plot of flow inclination angle versus yaw misalignment in high terrain roughness sector (30sec mean)

7. Conclusions

Application of a spinner anemometer for inflow measurements to a wind turbine rotor in wind farm environment was demonstrated. Calibration for angular measurements was made by yawing the wind turbine in and out of the wind in stopped condition, and calibration for wind speed measurements was made during operation by referencing a met mast in a free wind sector. Apart from calibration of the basic $k_{1,d}$ and k_2 constants an induction function with four constants was determined. The measurements of yaw misalignment showed good compliance with mast related wind measurements. This also confirms the flow inclination angle measurements which are equivalent to the yaw misalignment measurements. Standard deviation of measured wind speed showed good compliance with mast measurements. Turbulence measurements were overestimated by the spinner anemometer. However, correction of the measured wind speed at the spinner with the use of the induction factor correction function gave good compliance with mast turbulence measurements. This indicates that the smaller vortices in the air are not influenced by the overall reduced wind speed due to induction.

Yaw misalignment measurements showed an average yaw misalignment of about 10° and with a high scatter. A symmetric yaw misalignment pattern was found with yaw misalignments at about −10°. The cause of this might be due to the control system using the two symmetrically mounted sonic sensors on the nacelle in an alternating way. Flow inclination angle measurements were scattered around 0°, which should be expected for flat terrain, but with significant up and down flow in wakes of other wind turbines due to wake swirl. The largest wake swirl showed an

upflow of about 15° and a downflow of about −13° in the wake of the nearest wind turbine at 3.2D distance. Some flow inclination angles of −10° were seen in other sectors at high wind speeds, especially with flow from the close high terrain roughness village Tjæreborg. The turbulence measurements showed significant changes behind the wakes of the different wind turbines in the wind farm. Maximum turbulence of 0.25 was seen behind the nearest wind turbine at distance 3.2D, being reduced to 0.22 for a turbine at 4.3D and to 0.20 for turbines at 5.4-7.0D.

Acknowledgments

The funding support from the Danish EUDP research program and from Vattenfall are highly acknowledged.

References

[1] Pedersen T.F., *Spinner anemometry - an innovative wind measurement concept*, EWEC2007 Milan, 2007
[2] Pedersen T.F., Sørensen N., Enevoldsen P., *Aerodynamics and characteristics of a spinner anemometer*, Journal of physics: Conference Series 75 012018, 2007
[3] Pedersen T.F., Vita L., Sørensen N.N., Enevoldsen P., *Operational experiences with a spinner anemometer on a MW size wind turbine*, EWEC2008 Brussels, 2008
[4] Mikkelsen T. et.al., *A spinner-integrated wind lidar for enhanced wind turbine control*, Wind Energy, 2012
[5] Kragh K.A. et.al., *Precision and shortcomings of yaw error estimation using spinner-based light detection and ranging*, Wind Energy, 2012
[6] Højstrup J. et.al., *Maximize Energy Production by minimizing Yaw Misalignment - Large Scale Field Deployment of Spinner Anemometer*, EWEA2013 Vienna, 2012
[7] Wagner R. et.al., *Turbulence measurement with a two-beam nacelle lidar*, EWEA2013, 2013